

# 1 Surface air temperature variability in global climate models

2  
3 Richard Davy and Igor Esau

4 G.C. Rieber Climate Institute of the Nansen Environmental and Remote Sensing Centre,  
5 Bjerknes Centre for Climate Research, Thormøhlensgt. 47, 5006, Bergen, Norway.

6  
7 Correspondence to: [richard.davy@nersc.no](mailto:richard.davy@nersc.no)

8  
9 New results from the Coupled Model Inter-comparison Project phase 5  
10 (CMIP5) and multiple global reanalysis datasets are used to investigate the  
11 relationship between the mean and standard deviation in the surface air  
12 temperature. A combination of a land-sea mask and orographic filter were used  
13 to investigate the geographic region with the strongest correlation and in all  
14 cases this was found to be for low-lying over-land locations. This result is  
15 consistent with the expectation that differences in the effective heat capacity of  
16 the atmosphere are an important factor in determining the surface air  
17 temperature response to forcing.

## 18 19 1. Introduction

20 The surface air temperature (SAT) and its various properties (diurnal and seasonal range  
21 and extremes, trends and variability) are some of the most widely used metrics of global  
22 climate and climate change [IPCC AR4, 2007]. This is to be expected given SAT is such a  
23 readily measurable, and anthropically important, variable. The variability of the SAT at a  
24 given timescale is determined by three factors: the magnitude of the forcing, any feedback  
25 processes and the effective heat capacity of the system [Hasselmann, 1976]. Given the inverse  
26 dependency of the magnitude of changes in SAT on the effective heat capacity, some  
27 correlations between metrics of the SAT are anticipated to be innate to the thermodynamics of  
28 the climate system. For example, there is the strong positive correlation between SAT trends  
29 and variability across the globe, as has been shown in observations, reanalysis and CMIP3  
30 datasets [Esau et al., 2012]. This is to be expected given that SAT trends and variability are  
31 both manifestations of the magnitude of SAT response to forcing.

32  
33 The effective heat capacity of the atmosphere has been shown to be directly proportional to  
34 the depth of the planetary boundary layer (PBL) [Esau and Zilitinkevich, 2010]. The  
35 shallowest boundary-layers are found over land in locations with consistent negative surface  
36 sensible heat flux, leading to strongly stable thermal stratification. We can expect to see the  
37 strongest signal of PBL response at over-land locations. Since this mechanism is driven by the  
38 turbulent mixing that characterises the PBL we expect there to be a weaker relation between  
39 the temperature mean and variability in high-altitude locations where the PBL is exposed to  
40 the free atmosphere. There has been some indication that such patterns, predicted from PBL  
41 response theory, are constrained to the PBL from the work of Weber et al. [1994] but the  
42 reason for this was not identified. The prediction that this relationship between the mean and  
43 SD of SAT should be weaker in locations exposed to the free atmosphere allows us to falsify

44 the PBL-response mechanism by comparing correlations of mean and SD of SAT with and  
45 without the use of an orographic filter.

46

47 It has been established that the coldest locations have the greatest SAT variability [IPCC  
48 AR4, 2007], but a more general relationship between the mean and variability of SAT can be  
49 masked by specific geographical conditions. Here we have used a simple least-squares linear  
50 regression analysis to investigate the relationship between mean and standard deviation of  
51 SAT from CMIP5 results and various reanalysis datasets.

52

## 53 **2. Data sets**

54 The data used for this study were taken from the CMIP5 results and various global re-  
55 analysis projects, the data for which is hosted by the National Center for Atmospheric  
56 Research (NCAR). The temperature data were taken from the last 30 years of the ‘historical’  
57 runs of the CMIP5, and from the same years in the reanalysis datasets with the exception of  
58 the Japanese 25-year reanalysis project (JRA25) which is limited to 25 years.

59

60 The historical simulations of the CMIP5 are run using changing conditions consistent with  
61 observations including: atmospheric composition, including anthropogenic and volcanic  
62 influences; solar forcing; land use changes and emissions or concentrations of short-lived  
63 species and natural and anthropogenic aerosols [Taylor *et al.*, 2009]. These simulations are  
64 performed by coupled ocean-atmosphere global climate models. We have used results from 8  
65 of the groups that contributed to CMIP5: CSIRO Australia’s CSIRO Mk3.5 [Gordon *et al.*,  
66 2010]; the Japan agency for Marine-Earth Science and Technology and National institute for  
67 environmental studies MIROC-ESM-CHEM [Watanabe *et al.*, 2011] and MIROC5  
68 [Watanabe *et al.*, 2010]; the French national centre for meteorological research’s CNRM-  
69 CM5 [Voldoire *et al.*, 2012]; the UK Met Office Hadley Centre’s HadCM3 and HadGEM2-  
70 AO [Collins *et al.*, 2011]; the institute for numerical mathematics’ INMCM4 [Volodin, *et al.*,  
71 2010] and the Norwegian Climate Centre’s NorESM [Iversen *et al.*, 2012].

72

73 The reanalysis datasets used were: the JRA25; the National Centers for Environmental  
74 Prediction (NCEP) Climate Forecast System Reanalysis (CFSR); the European Center for  
75 Medium-range Weather Forecast (ECMWF) Interim reanalysis (ERA-Interim); the National  
76 Oceanic and Atmospheric Administration (NOAA) 20<sup>th</sup> century reanalysis v2 and the  
77 NCEP/NCAR reanalysis I.

78

## 79 **3. Methods**

80 Each of the global climate models and reanalysis has associated orographic data. An  
81 orographic filter, ‘Orog’, was created that removed all data corresponding to locations where  
82 the surface elevation is greater than 1 km. Locations with surface elevation greater than 1km  
83 (‘highland’) are assumed to be exposed to the free atmosphere. The land-sea mask of each  
84 dataset was used as a ‘land’ filter, to select only those grid-points which lay over land. The  
85 combination of the orographic and land filters was used to select only low-lying over-land  
86 (‘lowland’) locations, where we anticipate the strongest signal of the PBL-response.

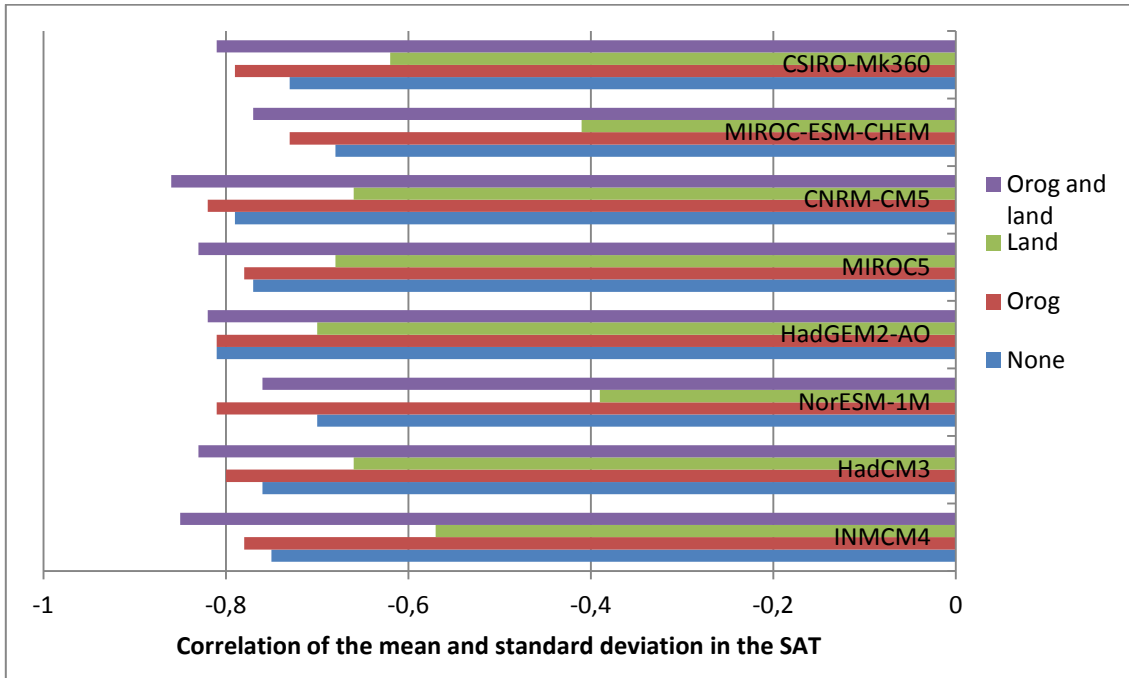
87

88 The monthly surface air temperatures were obtained for each dataset. A time-series of  
 89 temperature anomalies was calculated by removing the all-time monthly-means from the  
 90 temperature time series. The temperature statistics were calculated from the anomalies after  
 91 the removal of a 4<sup>th</sup> order polynomial trend from the series [Braganza *et al.*, 2003].  
 92

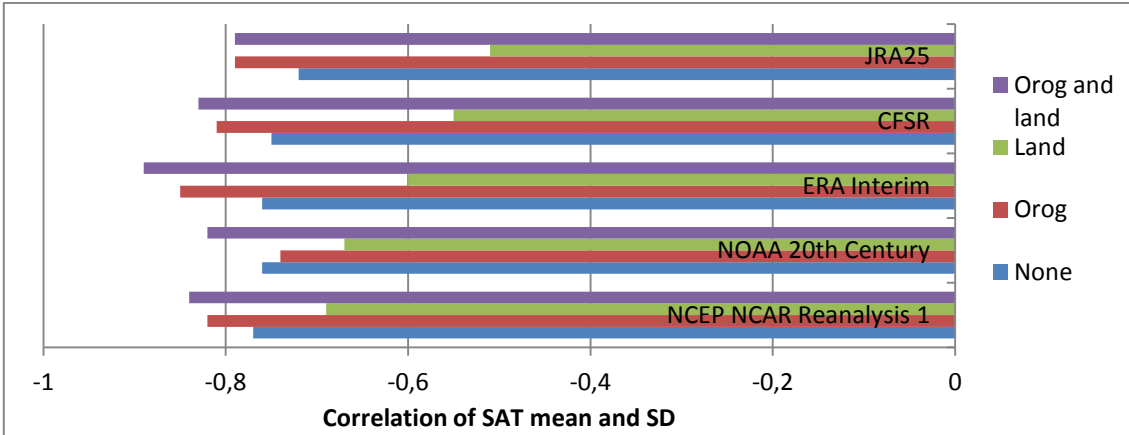
93 **4. Results**

94 Figure 1a shows the correlation of the mean and SD of the SAT from various global  
 95 climate models. Application of the orographic filter always improves the correlation and the  
 96 best correlations are found in lowland locations with the exception of the results from  
 97 NorESM where the over-land correlation is especially poor. We find the same result in the  
 98 reanalysis datasets with the strongest correlations always found for lowland locations (Figure  
 99 1b).

100  
 101



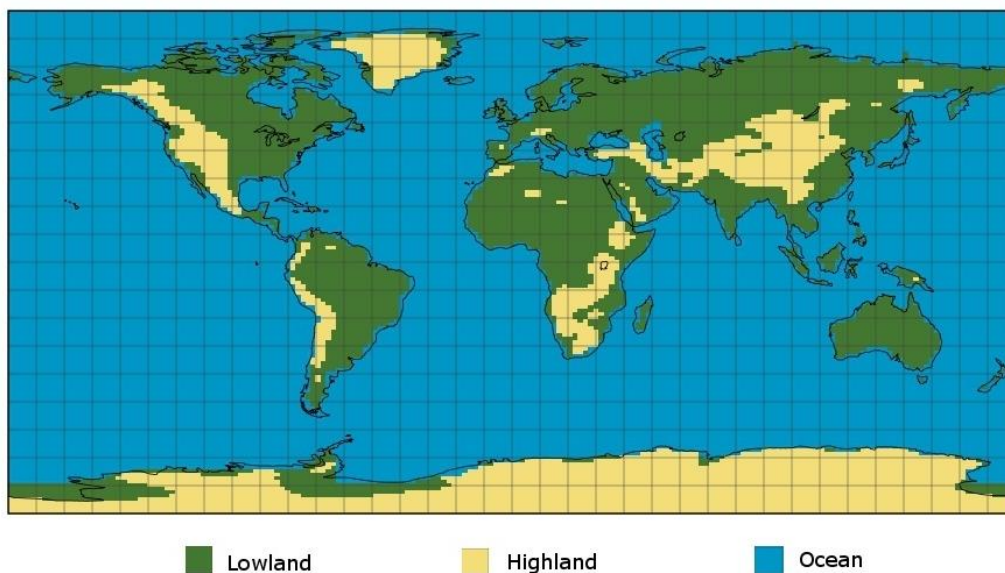
102



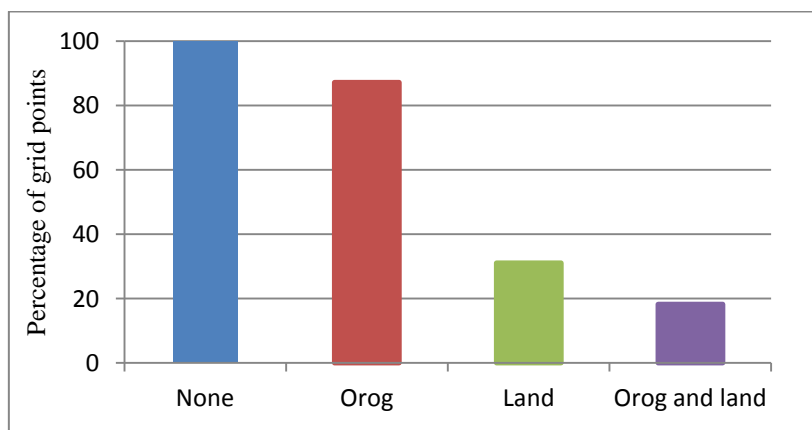
103  
 104

105 **Figure 1.** The correlation of the mean and standard deviation in surface air temperature from  
106 (a) CMIP5 models and (b) reanalysis calculated after applying a land-sea mask (land) and an  
107 orographic filter (Orog).  
108

109 In all cases the biggest difference in the correlation comes with the addition of the  
110 orographic filter to the land-filtered data. The significance of these differences in the  
111 correlations can be seen from the difference in the number of data points used in each case  
112 (Figure 2). The highland regions represent 13% of the total number of grid points so the  
113 addition of the orographic filter to the global data does not significantly improve the  
114 correlation. However, the highland locations represent 41% of the over-land grid points;  
115 hence the largest improvement in the correlations is seen in the application of the orographic  
116 filter to the over-land data. This is also why we see a drop in the correlation after the  
117 application of the land filter to the global data: the fraction of grid points which correspond to  
118 highland locations is increased.  
119



120  
121



122  
123  
124  
125  
126

**Figure 2.** a) Global distribution of regions of ocean, high land and low-lying land.  
b) The percentage of grid points remaining after applying the land and/or orographic filters.

127 **5. Conclusions**

128 In this study we used the results from the latest phase of the CMIP to identify one of the  
129 climatological signatures of SAT variability: the strong negative correlation between SAT  
130 mean and variability. This result was confirmed through analysis of multiple reanalysis  
131 datasets. This relation is consistent with the PBL-response hypothesis: that differences in the  
132 SAT variability are, in part, due to variations in the effective heat capacity of the atmosphere  
133 such that the lower the heat capacity the greater the SAT response to a given forcing [Esau et  
134 al., 2012]. When we include the highland locations where the PBL is exposed to the free  
135 atmosphere, and as such is not expected to produce the same response, we find a weaker  
136 correlation between the SAT mean and SD. This is in agreement with our expectation that this  
137 relationship is a consequence of the PBL response.

138  
139 **Acknowledgments.** This work has been funded by the Norwegian Research Council FRINAT  
140 project *PBL-feedback* 191516/V30.

141  
142 **References**

- 143 Balling Jr., R. C., P. J. Michaels and P. C. Knappenberger, (1998), Analysis of winter and  
144 summer warming rates in gridded temperature time series. *Clim. Res.*, **9**, 175-181, doi:  
145 10.3354/cr009175.
- 146 Beare, R. J., et al., (2006), An intercomparison of Large-Eddy Simulations of the stable  
147 boundary layer. *Bound.-Lay. Meteorol.*, **118**, 247-272, doi: 10.1007/s10546-004-  
148 2820-6
- 149 Braganza, K., et al., (2003), Simple indices of global climate variability and change: Part I,  
150 Variability and correlation structure. *Clim. Dyn.*, **20**, 491-502.
- 151 Collins, W.J., et al., (2011), Development and evaluation of an Earth-System model –  
152 HadGEM2. *Geosci. Model Dev.*, **4**, 1051-1075, doi: 10.5194/gmd-4-1051-2011.
- 153 Cuxart, J., et al., (2006), Single-column model intercomparison for a stably stratified  
154 atmospheric boundary layer, *Bound.-Lay. Meteorol.*, **118**, 273-303, doi:  
155 10.1007/s10546-005-3780-1
- 156 Easterling, D. R., et al., (1997), Maximum and minimum temperature trends for the globe,  
157 *Science*, **277**, 364-367.
- 158 Esau, I. and S. Zilitinkevich, (2010), On the role of the planetary boundary layer depth in the  
159 climate system. *Adv. Sci. Res.*, **4**, 63-69, doi:10.5194/asr-4-63-2010.
- 160 Esau, I., R. Davy and S. Outten, (2012), Complementary explanation of temperature response  
161 in the lower atmosphere. Submitted to *Env. Res. Lett.* Aug 2012.
- 162 Gordon, H.B., et al., (2010), The CSIRO Mk3.5 Climate Model, technical report No. 21, The  
163 Centre for Australian Weather and Climate Research, Aspendale, Vic., Australia.
- 164 Hansen, J., M. Sato and R. Ruedy, (1995), Long-term changes of the diurnal temperature  
165 cycle: implications about mechanisms of global climate change. *Atmos. Res.*, **37**, 175-  
166 209, doi: 10.1016/0169-8095(94)00077-Q.
- 167 IPCC, (2007), Climate Change 2007: The Physical Science Basis. Contribution of Working  
168 Group I to the Fourth Assessment Report of the Intergovernmental Panel on Climate  
169 Change [Solomon, S., D. Qin, M. Manning, Z. Chen, M. Marquis, K.B. Averyt,

170 M.Tignor and H.L. Miller (eds.)). Cambridge University Press, Cambridge, United  
171 Kingdom and New York, NY, USA.

172 Iversen, T., et al., (2012), The Norwegian Earth System Model, NorESM1-M – Part 2:  
173 Climate response and scenario projections. *Geosci. Model Dev. Discuss.*, **5**, 2933-2998.

174 Michaels, P. J., J. C. Balling Jr, R. S. Vose, P.C. Knappenberger, (1998), Analysis of trends in  
175 the variability of daily and monthly historical temperature measurements. *Clim. Res.*  
176 **10**, 27-33, doi: 10.3354/cr010027.

177 Taylor, K. E., R. J. Stouffer and G. A. Meehl, (2009), An overview of CMIP5 and the  
178 experiment design. *Bull. Amer. Meteor. Soc.*, **93**, 485-498.

179 Voltaire, A., et al., (2012), The CNRM-CM5.1 global climate model: description and basic  
180 Evaluation. *Clim. Dyn.*, doi: 10.1007/s00382-011-1259-y.

181 Volodin, E.M., N.A. Dianskii, A.V. Gusev, (2010), Simulating present-day climate with the  
182 INMCM4.0 coupled model of the atmospheric and oceanic general circulations.  
183 *Izvestiya Atmospheric and Oceanic physics*, **46** (4), 448-466.

184 Vose, R. S., D. R. Easterling, B. Gleason, (2005), Maximum and minimum temperature trends  
185 for the globe: An update through 2004. *Geophys. Res. Lett.* **32**, L23822.

186 Watanabe, S., et al., (2010), Improved climate simulation by MIROC5: Mean states,  
187 variability and climate sensitivity. *J. Climate*, **23**, 6312-6335, doi:  
188 10.1175/2010JCLI3679.1

189 Watanabe, S., et al., (2011), MIROC-ESM 2012: model description and basic results of  
190 CMIP5-20c3m experiments. *Geosci. Model Dev.*, **4**, 845-872, doi: 10.5194/gmd-4-  
191 845-2011.

192 Weber, R. O., P. Talkner, G. Stefanicki, (1994), Asymmetric diurnal temperature change in  
193 the Alpine region. *Geophys. Res. Lett.* **21**, 673-676.

194 Zilitinkevich, S. S., et al., (2008), Turbulence energetics in stably stratified geophysical flows:  
195 strong and weak mixing regimes. *Quart. J. Roy. Met. Soc.*, **134**, 793-799, doi:  
196 10.1002/qj.264.